Journal of Advanced Joining Processes 13 (2026) 100374

Contents lists available at ScienceDirect

Journal of Advanced Joining Processes

journal homepage: www.sciencedirect.com/journal/journal-of-advanced-joining-processes

Butt-joint welding process of PVC Profiles: Numerical modelling, experimental validation and insights into material behaviour and flow dynamics

Riccardo Panciroli [a], Daniele Chiappini [a], Roberto Palazzetti [b,*]

[a] Università degli studi Niccolò Cusano, Engineering Faculty, Rome, Italy
[b] Politecnico di Milano, Milano, Italy

ARTICLE INFO

Keywords:
PVC welding
Thermoplastic welding
Eulerian–Lagrangian simulations

ABSTRACT

Polyvinyl chloride (PVC) forming operations are typified by large deformations, free-surface condition, complex conjugate heat transfer, and intricate contact phenomena. This study focuses on numerical modelling of the forming process that occurs beneath the butt-joint welding of polymeric profiles to offer a comprehensive understanding of how process parameters and boundary conditions influence the final weld. Numerical simulations are based on arbitrary and coupled Lagrangian and Eulerian models, which incorporate viscoelasticity, heat transfer, external forces, and free-surface flow. Due to the extensive temperature range encountered during the process, during heating the material transitions from a linear elastic state to a low-viscosity fluid. Consequently, the model has been developed to simultaneously solve for both solid and free-surface fluid conditions, and PVC has been modelled as a temperature-dependent viscoelastic solid, exhibiting Newtonian-like fluid characteristics under high temperatures. The proposed numerical solution methodology is employed to offer insights into the physics of the butt-welding process, widely utilised within industry. Two distinct configurations have been modelled to study material flow during the process: with and without a rigid constrain that prevents the material from moving freely upwards. These simulations aim to illuminate the impact of boundary conditions and physical constraints on the welding process and material behaviour.

Introduction

The welding of thermoplastic polymers is a key process in numerous industrial applications, ranging from automotive to construction, owing to the materials' versatility, low cost, and ease of processing. Among these, polyvinyl chloride (PVC) is widely utilised due to its favourable mechanical and chemical properties. However, the inherent low thermal conductivity of PVC presents significant challenges during welding, often resulting in steep thermal gradients and the need for precise control of process parameters to ensure high-quality welds.

A significant impetus for the widespread use of PVC has been its ease of joining, achievable through a number of different processes and techniques (Jin et al., 2014). Numerous studies in the literature focus on the joining of thermoplastics in general, including PVC, through adhesives, fastenings, or welding (Silva et al., 2021). However, only few studies address the numerical simulation of such joining processes, particularly with respect to welding, which is the primary focus of this work.

Butt-joint welding is a common technique employed for joining thermoplastic profiles. This process involves heating the profile edges to their melting temperature, followed by pressing the molten surfaces together to form a strong joint upon solidification. While this method is effective, the complex interplay between heat transfer, material flow, and mechanical deformation makes the prediction and optimisation of welding outcomes highly challenging. The thermomechanical behaviour of PVC, which transitions from a linear elastic solid at room temperature to a low-viscosity fluid at elevated temperatures, further complicates the process.

Most of the research presented in the literature concerns the numerical modelling of thermoplastic welding, specifically using the Laser Transmission Welding (LTW) technique. Notably, significant contributions have been made by Prof. Van de Ven and his collaborators (Van De Ven and Erdman, 2007a,b,c,d). They developed a proprietary numerical model based on the first principles of heat transfer, employing the energy balance method to calculate the temperature at nodes within the material and perpendicular to the direction of laser travel. Additionally, the joining pressure at the interface between the two parts to be welded is considered. Their model accounts for radiation and

* Corresponding author.
E-mail addresses: riccardo.panciroli@unicusano.it (R. Panciroli), daniele.chiappini@unicusano.it (D. Chiappini), roberto.palazzetti@polimi.it (R. Palazzetti).

https://doi.org/10.1016/j.jajp.2026.100374
Received 17 October 2025; Received in revised form 5 December 2025; Accepted 6 January 2026
Available online 6 January 2026

convection to the surroundings, conduction within each material, and contact conduction between the two parts. This model has been shown to provide acceptable agreement with experimental validations in terms of welding depth.

While LTW is widely used, it is not always feasible or sustainable, making Friction Stir Welding (FSW) a more frequently preferred alternative. Researchers have developed three main approaches to model thermoplastic FSW, based on thermal analysis, structural mechanics, and Computational Fluid Dynamics (CFD) (Iftikhar et al., 2022). However, these models still lack accuracy due to the complexity of the physics involved in FSW, primarily stemming from the challenges in determining material properties during the process. Another viable method is Ultrasonic Welding (UW), in which thermoplastics are welded by concentrating heat at the interface through the application of ultrasound pulses (Bhudolia et al., 2020). Zhang et al. (2010) developed a Finite Element Method (FEM) model for UW that uses the generalised Maxwell solid model for thermoplastics, with temperature-dependent properties implemented via segment time–temperature equivalency equations. They performed simulations using ANSYS APDL and compared the results with experimental data, demonstrating good agreement. Tutunjian et al. (2020) proposed a variant of the classic process, called Differential Ultrasonic Spot Welding (DUS), which aims to reduce or eliminate spot marks. The authors modelled the process using an explicit mechanical 3D FEM analysis to assess the presence of focused friction due to slippage at the weld zone and to provide a comprehensive understanding of the dynamic deformation behaviour of the laminates.

The present work focuses on a different welding technique, the butt-joint welding process, that is suitable for thermoplastics such as PVC, and commonly used in the window-making industry. PVC windows are built by butt-welding bars at the window's corners, and it is a delicate process, that must ensure strength as well as meet aesthetic standards. Performing a good weld is crucial for the product, and aim of this paper is to dig into the process and provide useful informations on how parameters affect the final outcome. This technique involves the use of heated blade(s) that bring the two mating surfaces to be joined slightly above their melting point. Once the surfaces reach the optimal temperature, the heating blade is removed, and the surfaces are brought into contact and pushed together. As the temperature cools, the two parts become firmly joined. To the best of the author's knowledge, no other work currently exists in the literature addressing the numerical modelling of this process, relevant also for a number of different applications, such as pipes, and plastic frames. This gap in the literature is the focus of the present study.

More in detail, we present a multiphysics numerical model for simulating the butt-joint welding process of PVC profiles. The model incorporates the coupled effects of heat transfer, viscoelastic deformation, and free-surface flow to capture the complex behaviour of PVC across a wide temperature range. By solving the simultaneous solid and fluid mechanics of the material, the model provides detailed insights into the influence of various process parameters on weld quality.

A critical aspect of the butt-joint welding process is the aesthetic and functional quality of the weld. The formation of visible defects, such as material overflow or incomplete fusion, can significantly impact the overall quality of the joint. Process parameters such as heating time and mating velocity have been identified as key factors influencing weld quality. Despite extensive experimental studies on thermoplastic welding, the high cost and time associated with physical trials highlight the need for predictive numerical models to optimise the process efficiently.

The numerical framework is applied to investigate the effects of mating velocity, heating time, and the presence of rigid walls on the weld's morphology and integrity. Furthermore, experimental validation of the model is conducted through collaboration with GRAF Synergy, an industry partner specialised in thermoplastic welding technology. The experimental data, obtained using a modified industrial welding machine, are compared with numerical predictions to assess the model's accuracy and reliability.

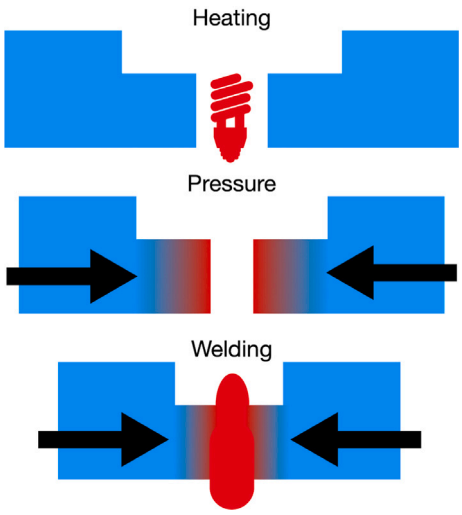

Fig. 1. Schematic representation of the PVC welding process from top to bottom: (1) heating phase; (2) mating phase to bring samples into contact; (3) welding phase.

The findings of this study underscore the importance of numerical simulations as a powerful tool for optimising the welding process of thermoplastic materials. By providing a deeper understanding of the underlying physics, this work contributes to the development of more efficient and reliable welding methodologies, ultimately enhancing the performance and durability of thermoplastic joints.

Problem assessment

This work addresses the butt joint welding process of PVC bars. Gaining a deeper insight into the physics underlying this process and developing a predictive tool is of great interest to the industry, as it is employed in a wide range of applications. The butt joint welding of polymeric profiles is an extremely common process. Similar to other polymers, PVC welding does not involve the introduction of external material, as the joining mechanism relies on autoadhesion (Vendan et al., 2019); that is, the original material of the components being welded forms the welding bevel.

Fig. 1 shows a schematic representation of the butt joint welding process for two PVC bars, which present a chamfer on the upper surface, the role of which is detailed later. The figure illustrates the main operations required to perform the butt welding of a thermoplastic polymeric profile. In the first phase, the two polymeric profiles are heated above the melting temperature using a heating blade. The heated material then forms the welding bevel. In the second phase, the heating blade is removed, and the two polymeric profiles are advanced to mate and initiate the welding process. During this phase, no additional heat is introduced, and the temperature drops rapidly, leading to the re-solidification of the material. It is crucial to mate the profiles within a short time to avoid local inconsistencies. Finally, in the third phase, the two profiles are pressed together to form the butt joint. The molten material flows, and the primary aim of this work is to assess the influence of process parameters on the propagation of the material.

As previously described, PVC bars are typically butt-welded using a hot blade, with its temperature adjusted to be as high as possible to minimise overall welding time. However, it is kept low enough to minimise the emission of Hydrochloric Acid (HCl), which is hazardous to both people and the environment. Unless specific strategies are

implemented in the welding process, a portion of the molten material may flow over the external surface, compromising the aesthetics of the weld. A mechanical process is then required to finalise the weld.

An outstanding example where the aesthetics of the weld are paramount is in the production of PVC window frames, which are composed of a series of butt-joined profiles. One of the most commonly employed strategies to finalise the welding is to mechanically remove the excess material before the welding starts, typically through a millimetre-sized square or angled chamfer. Chamfering plays an essential role in improving the aesthetics of the welded joint also by confining the excess molten PVC expelled during welding and therefore reducing or eliminating for post-weld trimming, which is undesirable because it leaves visible marks on the frame. Although PVC profiles are cut at 45° to produce a final 90° corner, this machining step does not alter the welding mechanism. The two profile ends are aligned without relative shear motion, and the process remains a true head-to-head welding, regardless of the angle at which the profiles meet. Another viable strategy to improve the aesthetics of the weld is to optimise the welding process itself, guiding the molten material to flow in prescribed directions so that the bead weld is hidden within, or grows in specific areas. One of the objectives of this work is to model the material's behaviour during the welding process and to identify the factors that drive its flow.

The operative settings considered in this study are relevant to industrial applications, particularly the welding of PVC profiles in the window-making industry. These parameters include the heating temperature, which ranges from 240 to 250 °C, the mating velocity, which under operating conditions falls between 0.05 and 0.4 mm/s, and the heating time, which is in the order of 30 s. Since these parameters are numerous and tuned as a function of the operative conditions specific to each machine and vary with the shape of the mating profiles, it is impractical to study the variation of all of them comprehensively. We will therefore focus on a given profile geometry, fixing the heating blade temperature to 250 °C, while investigating the influence of the most relevant parameters affecting the quality of the weld, such as the mating velocity and the boundary conditions.

PVC material behaviour

The mechanical properties of PVC are highly temperature-dependent. When the temperature of PVC is below its glass transition temperature (T_g), around 80 °C, the polymer is hard and brittle, exhibiting the characteristic behaviour of rigid plastic materials. However, when the polymer is heated above T_g, it may undergo large deformations under the action of a constant load. Its behaviour transitions from glassy to rubbery, that is, from a brittle, purely elastic response to a viscoelastic one (Tomaszewska et al., 2021).

The viscoelastic behaviour of PVC consists of both instantaneous deformation (elastic effect) and continuous deformation (viscous effect), with the latter varying over time. The viscous and elastic properties of the polymer vary within the temperature range of 77 °C to about 250 °C, with viscosity decreasing significantly as temperature increases. Moreover, below a certain shear rate, molten PVC behaves as a Newtonian fluid, while at higher strain rates, typically of the order of 10^{-1} s^{-1}, strain rate effects emerge. In this regime, the viscosity decreases with increasing shear rate, similar to shear-thinning non-Newtonian fluids (Cao et al., 2019). In this paper the PVC viscosity has been modelled through a simplified approach which takes into account only the temperature variation, as better detailed in the following section.

The upper temperature limit to which PVC can be heated depends on the polymer's degradation rate, which increases with temperature. The threshold for initial decomposition occurs at approximately 257 °C (Kök et al., 2008; Nisar et al., 2018). The viscous characteristics of PVC are closely related to the shear rate and are also responsible for creep. Creep is a mechanical phenomenon in which strain gradually increases with time under a constant load. Even though the deformations in molten PVC are primarily governed by viscous flow, the material still maintains a non-negligible stiffness, and elastic deformations can be significant as well. Therefore, the material model for PVC at high temperatures behaves as a combination of a solid and a viscous fluid.

Numerical model

The welding process of polymers falls within the domain of thermomechanical coupling, as it involves not only heat transfer but also mechanical forces that must be accounted for. In the specific process under consideration, heat transfer is predominantly governed by conduction via the heating tool, with only a minor contribution from convection and radiation. In this study, the effects of convection and thermal radiation are disregarded, as they are assumed to be negligible in comparison to conduction.

A significant challenge in the numerical modelling of the problem addressed herein lies in the simultaneous handling of a moving free-surface boundary associated with very large deformations and self-penetration phenomena. Furthermore, the analysis must account for a wide temperature range, which results in a structural behaviour transitioning from a linear elastic solid at lower temperatures to a low-viscosity fluid at elevated temperatures. Consequently, the numerical model must be capable of concurrently solving for both solid mechanics and free-surface fluid dynamics.

To address this complex problem, a Finite Element Method (FEM) numerical model was implemented, employing an Arbitrary Lagrangian–Eulerian (ALE) framework (Braess and Wriggers, 2000). This approach enables the tracking of the extensive deformations exhibited by the melting polymer. The commercial software LS-DYNA (R11.2.2) was utilised for this purpose, as it provides the capability to interface material flow within ALE meshes with Lagrangian elements. This facilitates the imposition of rigid or flexible moving boundaries and allows for the execution of fully coupled fluid–structure interaction simulations.

Numerical modelling of PVC at high temperatures

Several models are available for the study of non-Newtonian fluids. Broadly speaking, the viscosity of polyvinyl chloride (PVC) is influenced by either the local strain rate or the temperature, the latter affecting the zero-shear-rate viscosity. In the extensive field of pseudo-plastic modelling, one may consider the Herschel–Bulkley or Bingham plastic models (Alexandrou et al., 2001; Moreno et al., 2016), both of which are highly versatile despite requiring the introduction of several parameters. Alternatively, the simpler Carreau model for pseudo-plastic behaviour may be employed, where a plateau viscosity is specified to address very low shear rates (Nakayama, 2018).

To simplify the modelling approach, preliminary analyses conducted on simplified numerical representations of the welding process indicated that the particular welding process studied here involves shear rates on the order of 10^{-1} s^{-1}. In principle, the analysis of a non-Newtonian viscoelastic fluid should account for interactions related to shear stress in order to accurately estimate the viscosity. However, the relatively low shear stress values typical of this application allow for reducing this degree of freedom, simplifying the model effectively. The implemented model considers only the variation of viscosity with temperature, as the effect of strain rate is negligible compared to that of temperature. This approach is supported by previous findings (Cao et al., 2019), which demonstrated that viscosity becomes significantly influenced by the shear rate only beyond a threshold of 10^{-1} s^{-1}.

As illustrated in Fig. 2, within the temperature range of interest (160 to 250 °C), the viscosity exhibits variations spanning four orders of magnitude. In contrast, multiple orders of magnitude of shear rate variation are required to reduce the viscosity by just one order of magnitude. Consequently, for the case under investigation—characterised by

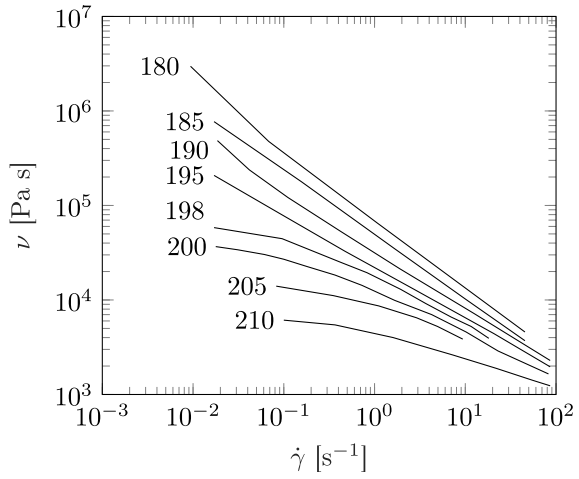

Fig. 2. Variation of PVC viscosity as a function of temperature and shear rate. *Source:* Reconstructed from the data reported in Münstedt (1977, 2021).

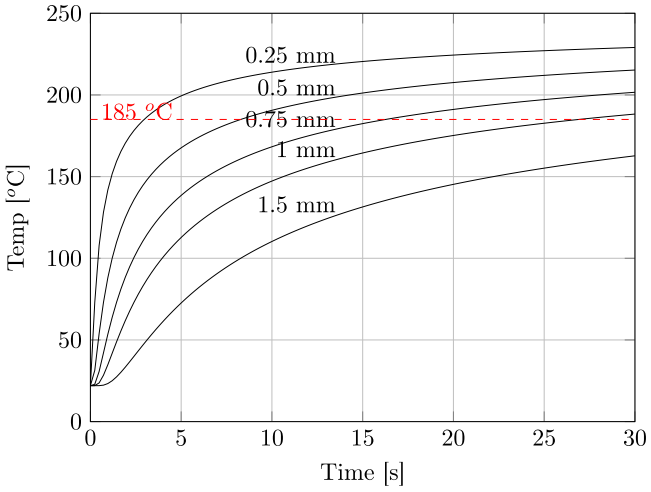

Fig. 3. Time trace of temperature at selected locations during the heating phase—analytical solution from the 1D heat equation. Distance is measured from the heating blade.

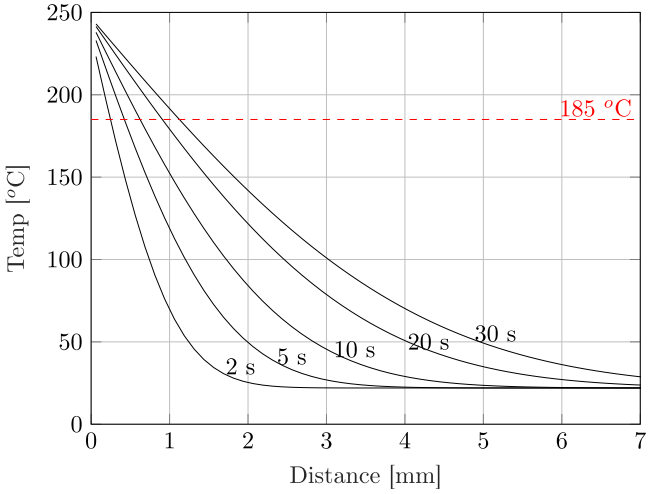

Fig. 4. Temperature profiles over the specimen at selected times—analytical solution from the 1D heat equation.

substantial temperature variations but relatively low shear rates—PVC can be effectively modelled as a temperature-dependent viscoelastic solid exhibiting Newtonian-like fluid behaviour.

To accurately model this unique mechanical behaviour, the material model must incorporate the combined response of a non-Newtonian fluid and an elastic solid (Snoeijer et al., 2020). For this purpose, we utilised `*MAT_60`, a material model available within the commercial software LS-DYNA, originally developed for simulating the forming of glass products (e.g., car windshields) at elevated temperatures. This model represents the total deviatoric strain rate as the sum of elastic and viscous components, expressed as

$$\dot{\varepsilon}'_{tot} = \dot{\varepsilon}'_{ela} + \dot{\varepsilon}'_{vis} = \frac{\sigma'}{2G} + \frac{\sigma'}{2\nu(T)} \tag{1}$$

where ν is the temperature-dependent viscosity, which is here approximated through the Modified Cross Model as Altinkaynak et al. (2011), Chiang et al. (1991), Bovo et al. (2024):

$$\nu(T) = (1.086 \cdot 10^9) \exp\left(\frac{-24.753(T - 373.15)}{51.6 + (T - 373.15)}\right) \text{[Pa s]} \tag{2}$$

This equation aligns well with data available from the literature. However, it predicts exceedingly high viscosity values at low temperatures. For instance, the viscosity decreases from an order of magnitude of 10^{16} at 80 °C down to 10^1 at 250 °C. Such a drastic variation poses significant challenges for numerical solvers, which tend to experience instability under these conditions. To address this, the variation of viscosity follows Eq. (2) but with upper bound imposed to restrict the viscosity within the range 10^{11} – 10^1. This bounded approach ensures numerical stability while maintaining fidelity to the material's behaviour.

To finalise the material data input, the following properties were assigned as constants across the entire temperature spectrum: a density of 1420 kg/m^3, an elastic modulus of 3.0 GPa, a specific heat capacity of 880 J/(kg K), and a thermal conductivity of 0.22 W/(m K).

Some insights on the conductive heating of PVC

An estimation of the temporal evolution of temperature along the sample can be obtained by solving the heat equation, which, under the approximation of one-dimensional (1D) conditions, is expressed as

$$\frac{dT}{dt} = \alpha \frac{d^2T}{dx^2}, \tag{3}$$

where α represents the thermal diffusivity, approximated as $\alpha = k/(\rho c_p)$, with k, ρ, and c_p denoting the thermal conductivity, mass density, and specific heat capacity, respectively.

The heat equation is solved over a spatial domain of 5 mm, with the following conditions applied: $\alpha = 1.76 \cdot 10^{-7}$ m^2/s, an initial uniform temperature of 22 °C, and a boundary temperature of 250 °C on the heated side. The boundary temperature of 250 °C was selected as it falls within the effective operative conditions of actual PVC-welding machines relevant to industrial applications, which usually range in between 240 to 250 °C, bing the latter the maximum operational temperature before the onset of excessively rapid polymer degradation.

Fig. 3 illustrates the evolution of temperature over time at selected distances from the heating blade, based on the solution of the 1D heat equation. Similarly, Fig. 4 depicts the spatial distribution of temperature at selected time intervals corresponding to the same solution.

It is worth noting that the propagation of heat within PVC is exceptionally slow due to its low thermal diffusivity. As observed in Fig. 2, the viscosity decreases below 10^6 Pa s only at temperatures exceeding 185 °C. Assuming that at least 1 mm of material must be softened to facilitate the welding process, Fig. 4 suggests that a minimum heating time of 25 s is required to adequately prepare the mating surfaces.

This estimated value should be interpreted as theoretical, given that the welding process necessitates the removal of the heating blade

before joining the profiles. During this transition, the PVC experiences a temperature drop. Consequently, a heating time of 30 s has been arbitrarily imposed, followed by a 2-second waiting period before the joint is executed. Notably, such a heating time of 30 s matches with the operative conditions actually utilised in industrial applications.

Numerical model implementation

All numerical analyses were conducted using a two-dimensional (2D) model under plane-strain conditions, as the beam here considered has rectangular cross-section. The characteristic dimensions of the profile cross-section used here do not match the proprietary industrial geometries (which are protected), but they are very close in shape and scale, ensuring that the mechanical behaviour is faithfully reproduced while respecting intellectual-property constraints.

The single-material plus void formulation was selected for the Arbitrary Lagrangian–Eulerian (ALE) elements. The ALE domain was discretised into a uniform grid with a characteristic element size of 12.5 μm, resulting in a total of 56,000 elements. Given that the PVC profile has a thickness of 2 mm, this corresponds to 160 elements through the thickness.

Elements representing the initial form of the PVC profile were activated with the viscoelastic material model, while elements corresponding to the external environment were designated as void. An alternative approach could have involved employing the multi-material formulation and assigning material properties for the surrounding air. However, the single-material plus void strategy was preferred as it minimises computational cost.

The problem under consideration includes an initial phase where only thermal loads are applied. Mechanical deformation begins after 20 s, when a low compressive force is exerted on the profile as it is pushed against the heating blade. The purely thermal portion of the analysis was solved using an implicit formulation, with a fixed timestep of 0.1 s applied to both the structural and thermal solvers.

Subsequently, the solution transitioned to an explicit formulation, as this was determined to be the only viable approach for accurately capturing the large viscous deformations involved. During the explicit phase, the thermal timestep was reduced to 0.01 s. This reduction was necessary to accurately track the material flow under the given conditions.

Boundary and loading conditions

The schematic shown in Fig. 5 illustrates the general implementation of the numerical model, highlighting the polymer in its initial configuration, the surrounding air (modelled as void), and the boundary conditions applied along the outer boundary, Γ. Within the model, the polymer is constrained to flow from the left boundary (inlet) towards the right with an imposed velocity matching the desired time-displacement curve. A symmetry boundary condition has been applied to the right edge of the domain, which initially corresponds to the heating blade during the heating phase and subsequently serves as a symmetry boundary for the remainder of the simulation. This approach enables the modelling of only one of the two components to be welded.

It is noteworthy that the edge of the polymer profile intended for contact with the heating blade—and subsequently forming the welding surface—is not cut planar. Instead, it incorporates a square chamfer. This specific geometry was chosen as it is hypothesised to enhance the quality of the final welding surface, especially in cases where aesthetic optimisation is required for the top surface, as illustrated in Fig. 5. In conventional welding of PVC bars, one of the two external surfaces remains visible, while the opposite one is hidden on the inner side the manufactured. The case presented here makes no exception: the chamfer is located in the visible side and is designed also to ensure good aesthetic to the joint. Further analysis of the chamfer's influence on welding quality is provided in the next section.

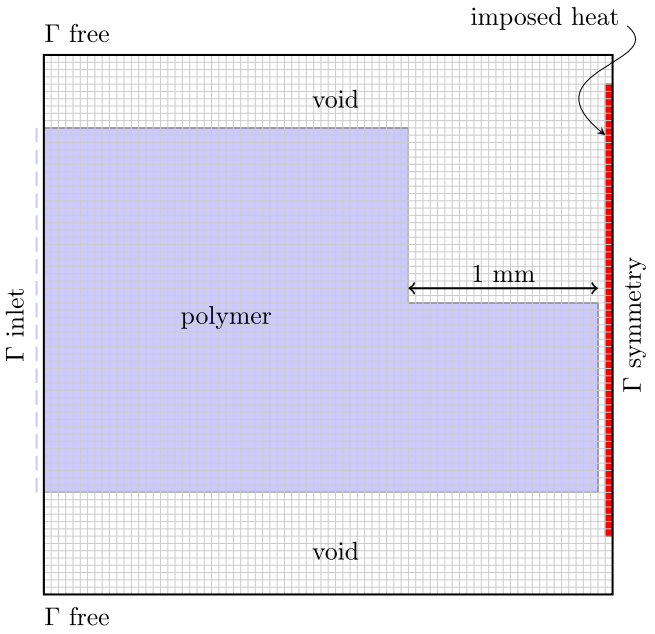

Fig. 5. Schematic of the numerical model with highlighted boundary conditions.

As outlined in Section "Introduction", the welding process comprises an initial heating phase where a blade, maintained at a high temperature, comes into contact with the edges of the profiles to be welded. During this phase, the profiles are slightly pushed against the heating blade. Following this, the blade is removed, and the profiles are pressed together to complete the welding process.

In the numerical model, the heating tool itself is not explicitly represented. Instead, the time-dependent heat transfer is applied directly to the nodes along the symmetry boundary. Specifically, a temperature of 250 °C is imposed on these nodes during the heating period using the `*BOUNDARY_PRESCRIBED_TEMPERATURE` keyword, with a deactivation time of 30 s.

The mating motion that joins the two profiles is implemented by applying an inlet boundary condition along the left edge of the domain, as illustrated in Fig. 5. A prescribed motion is imposed on the nodes initially associated with the PVC material. The motion of the PVC is programmed such that it remains stationary during the initial heating phase. Subsequently, it advances by 0.25 mm at a constant rate of 0.025 mm/s during the final portion of the heating phase, specifically between 20 and 30 s. This movement is then paused for 2 s, representing the period during which the heating blade is removed and the profiles are aligned for welding. The welding process itself is executed by imposing a continuous, steady advancing movement. The final quality of the weld is influenced by a wide range of process parameters, each contributing to the thermal and mechanical conditions experienced by the material during joining. While the heating time, heating temperature, and geometric configuration are fixed in the present analysis, several other factors remain open for investigation. Among these, the waiting time between the removal of the heating blade and the onset of mating and the velocity at which the profiles are brought into contact are particularly relevant. In this study, we specifically focus on the influence of the mating velocity, which is a key parameter governing the temperature distribution, material flow, and ultimately the effectiveness of the weld. For this reason we will particularly focus on the effect of different mating velocities. The time-displacement motion curve is presented in Fig. 6, alongside the imposed temperature over time.

A preliminary sensitivity analysis has been conducted to assess the impact of the timing parameters on the final weld quality and material

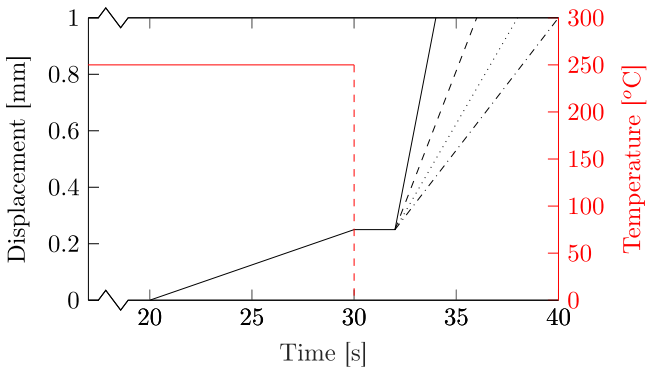

Fig. 6. Prescribed motion imposed to the nodes on the left boundary associated to PVC only (Γ inlet), and imposed temperature on the nodes on the symmetry plane. Solid, dashed, dotted, and dashdotted lines correspond to a final advancing ratios of 0.375, 0.185, 0.125, and 0.093 mm/s, respectively.

flow. The results of this analysis indicate that the advancing ratios and timings during the heating phase have a negligible effect on the visible portion of the weld. However, the initial mating speed does influence the material distribution in the lower area, which remains invisible to the eye. As this region is not of primary concern, it will not be discussed further; additional details can be found in Appendix Section "Effect of advancing velocity during the heating phase" for those interested. In contrast, the advancing velocity during the second phase of the weld (when the profiles are mated) does have an impact on the weld quality, and this aspect is discussed in greater detail in the following section.

To evaluate the impact of the advancing velocity on the quality of the weld, we investigated four different advancing velocities falling within the actual operative range utilised in industrial machines, namely: 0.375 mm/s, 0.185 mm/s, 0.125 mm/s, and 0.093 mm/s. These conditions are depicted in Fig. 6 using solid, dashed, dotted, and dash-dotted lines, respectively. It is important to note that the four mating velocities analysed in the main body of this work do not represent the entirety of the simulations performed. A broader parametric study has also been conducted, as detailed in Appendix Section "Optimal combination of dwell time and mating velocity", where an extended range of mating velocities is considered. In that complementary analysis, the focus shifts towards exploring the combined effect of dwell time—defined as the delay between the removal of the heating blade and the onset of mating—and the mating velocity itself. The objective of this expanded investigation is to identify the optimal process window that ensures a high-quality weld, balancing the need for sufficient temperature retention with adequate material flow. This additional study reinforces the significance of thermal management and motion synchronisation in achieving structurally sound and aesthetically acceptable welds.

The following section presents the simulation results, with particular emphasis on the influence of mating velocity on the final weld quality. Additionally, an alternative welding process is explored, involving the introduction of a rigid wall along the upper boundary, which can be either fixed or moving with the profile, as shown in Fig. 7. This wall prevents the upward flow of polymer, thereby improving the aesthetic quality of the weld and potentially eliminating the need for a subsequent machining process.

Results and discussion

This section details the effect of the mating velocity and the presence of the rigid wall on the quality of the welding surface in terms of both aesthetics and functionality.

Open condition

The initial focus is directed towards analysing the morphology of the weld. Fig. 8 depicts the free surface of the polymer at selected time intervals during the welding process for various advancing velocities. In all cases, the solution remains self-similar up to 32 s, as the heating phase is identical across the simulations. However, as the process progresses, the morphology of the weld is observed to be significantly influenced by the advancing velocity.

It is worth noting that the mating velocity affects the temperature of the welding bead. Specifically, the overall temperature at the end of the welding process increases with higher advancing velocities. This results in a lower viscosity for the PVC when welding is performed at greater speeds, as higher velocities facilitate the flow of the material, particularly within the chamfer region.

As shown in Fig. 8, welds produced at higher advancing velocities exhibit a surface characterised by a considerable amount of material overflowing both the top and bottom surfaces. In such cases, post-weld machining would likely be required to improve the aesthetic quality of the weld. Conversely, as the advancing velocity decreases, the material's resistance to flow increases, leading to a reduction in the amount of material trickling over the upper and lower surfaces. This results in a noticeable improvement in the weld's aesthetic quality.

However, at lower advancing velocities, a potential drawback arises: the material initially located within the chamfer region—which is intended to form the welding bead—may not flow sufficiently to fill the entire gap. In such scenarios, the uppermost portion of the weld may consist of the two original profiles in direct contact, without any melted material interposing between them. This outcome is strongly influenced by the temperature, as slower advancing velocities allow the material to cool excessively before the welding is completed.

This effect is further illustrated in Fig. 9, which presents the temperature distribution at selected time intervals for representative velocities of 0.375 and 0.125 mm/s. At the conclusion of the heating phase (30 s), the temperature distribution reveals that the material within the chamfer has been heated to a temperature exceeding 200 °C, resulting in low viscosity. As the heating blade is removed, the temperature drops rapidly, leading to an increase in viscosity.

If the profiles advance quickly, the material can smoothly flow over the surfaces to be joined before solidification occurs. As shown in Fig. 9, the temperatures within the flowing material remain above 200 °C at the end of the mating process in this case.

Conversely, if the advancing velocity is too slow, the PVC becomes too viscous to effectively flow over the entire mating surface, and the upper portion of the material remains dry. In such cases, the upper parts of the profiles may eventually make contact, but without forming a proper weld. The temperature distribution in this scenario indicates that, at the end of the mating process, the temperatures in the upper section of the weld have dropped below 180 °C, corresponding to a high viscosity that hinders material flow. Notably, the temperatures remain slightly higher in the material moving downward, which leads to a concentration of material in that direction.

Rigid wall condition

The presence of the rigid wall on the upper surface exerts a significant influence on the aesthetic quality of the weld, while similar effects can also be observed in terms of its functional performance. Fig. 10 depicts the free surface of the polymer at selected time intervals during the welding process for varying advancing velocities.

The role of the rigid wall is twofold:

- At lower final viscosities (associated with higher mating velocities and thus elevated temperatures), the rigid wall serves as a confinement barrier, preventing the polymer from flowing excessively over the wall.

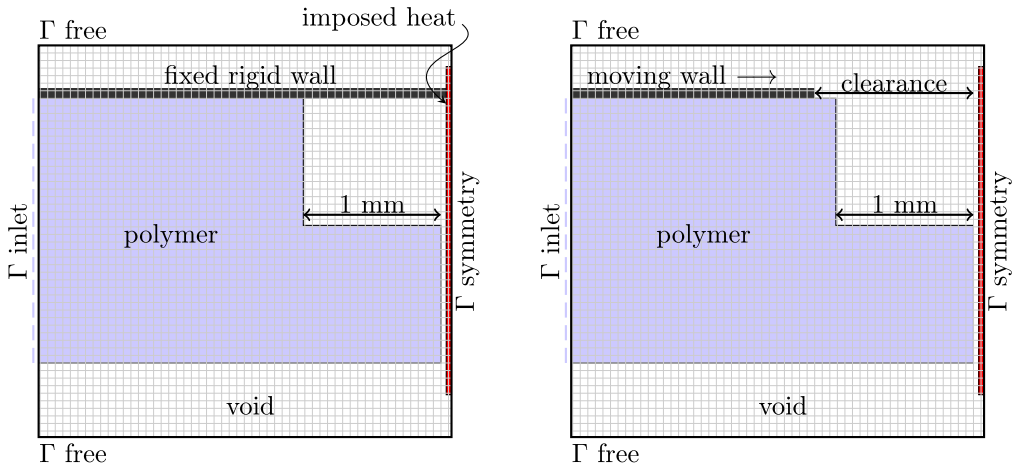

Fig. 7. Schematic of the numerical model with highlighted boundary conditions for the case where a fixed (left) or moving (right) rigid wall is mating the top surface.

- At higher final viscosities (resulting from slower mating velocities and reduced temperatures), the rigid wall acts to restrict the upward movement of the profile's upper surface. This containment effectively "closes" the chamfer region, ensuring that the molten PVC remains confined within the mating profiles.

As a result, the upper surface of the weld remains flat and smooth over a broad spectrum of process parameters.

As previously discussed, if the advancing velocity falls below a certain threshold, the material is unable to flow upwards to the rigid wall and instead predominantly flows downward. Consequently, the upper portion of the weld becomes a dry spot, which adversely affects the mechanical properties of the weld.

Among the four advancing velocities examined in this study, only the first two are capable of producing an effective weld, whereby advancing velocities below 0.185 mm/s are instead predicted to introduce a dry spot. However, it is worth to stress that such a specific velocity is only relevant to this exact geometry and process parameters. Fig. 11 shows the temperature distribution in the weld bead for this case. Notably, the temperature at the topmost part of the weld at the end of the mating process is just above 200 °C. Had the temperature dropped below this threshold prior to completing the weld, the process would have failed.

Moving wall

For completeness, it should be noted that the numerical simulations also investigated a third scenario in which the upper rigid wall was not stationary but instead modelled as a rigid boundary with prescribed motion, moving in synchrony with the profile. The results for this case are not extensively reported for the sake of brevity, as the moving boundary was found to produce effects identical to those observed with the stationary rigid wall, with reference to the ability of the moving blades to confine the material within the bead. Nevertheless, it is important to highlight that the initial position of the moving rigid wall must allow sufficient clearance from the heating blade (and, by extension, the welding centre), as the motion of the rigid wall exceeds that of the polymer in the molten zone.

Specifically, while both the moving wall and the polymer are driven together towards the symmetry plane, the cold (and therefore stiff) polymer moves at the same speed as the rigid wall, whereas the molten polymer deforms backwards relative to the wall's motion. As a result, the moving wall progresses more rapidly than the edge of the chamfer region. Adequate clearance must thus be ensured to prevent the moving wall from making contact with its counterpart on the opposite side of the symmetry plane before the welding process is fully completed. Fig. 12 presents two examples comparing the rigid and moving wall approaches. For brevity, other investigated cases are not shown.

Validation of the numerical model against experimental data

The numerical model developed in this study has been verified against experimental data obtained in collaboration with the company GRAF Synergy. The company granted us access to one of their production machines, allowing us to modify the grips and program the process parameters to perform experiments in accordance to the numerical scheme. This collaboration was essential to validate the numerical scheme and assess its predictive capabilities in replicating real-world welding outcomes.

Given the proprietary nature of the welding process employed by GRAF Synergy, whereby all the experimental conditions are very similar to what implemented numerically and accurately detailed in the previous sections, only a limited subset of data is presented here. The heating blade has been set to 240 °C and the mating velocity to 0.2 mm/s, as these represent the central values within the range used in actual applications, while chamfer dimensions remain confidential and cannot be disclosed publicly. The verification presented here focuses on comparing the final cross-sectional profiles of the welds obtained through simulations with those observed experimentally.

The experimental process involved heating the PVC profiles to the target temperature, followed by welding at controlled mating velocities. The final cross-sections of the welded joints were captured through precise cutting and imaging of the profiles, ensuring an accurate representation of the weld geometry for comparison with the numerical results. Key features, such as the weld bead morphology, the presence of dry spots, and the extent of material overflow, were extracted and compared to the numerical predictions.

The experiments were conducted for various positions of the containment blade (the moving rigid wall in the simulations), specifically located at a distance from the chamfer border of 0 mm, 0.3 mm, 0.5 mm, and 2.5 mm (representing the open condition). These configurations allowed for a comprehensive evaluation of the model's ability to predict the material flow and weld morphology under different boundary constraints. Typical examples of the weld cross-section vor the several cases under exam are presented in Fig. 13. The numerical model demonstrated remarkable agreement with the experimental results, effectively capturing the morphological features of the weld across all tested configurations. The comparison highlighted the model's ability to predict material flow and the resulting weld geometry under different boundary constraints. The good correlation between simulation and experimental observations underscores the robustness and applicability of the numerical scheme to industrial welding processes. This validation reinforces the potential of the model as a tool for optimising welding parameters and improving process outcomes.

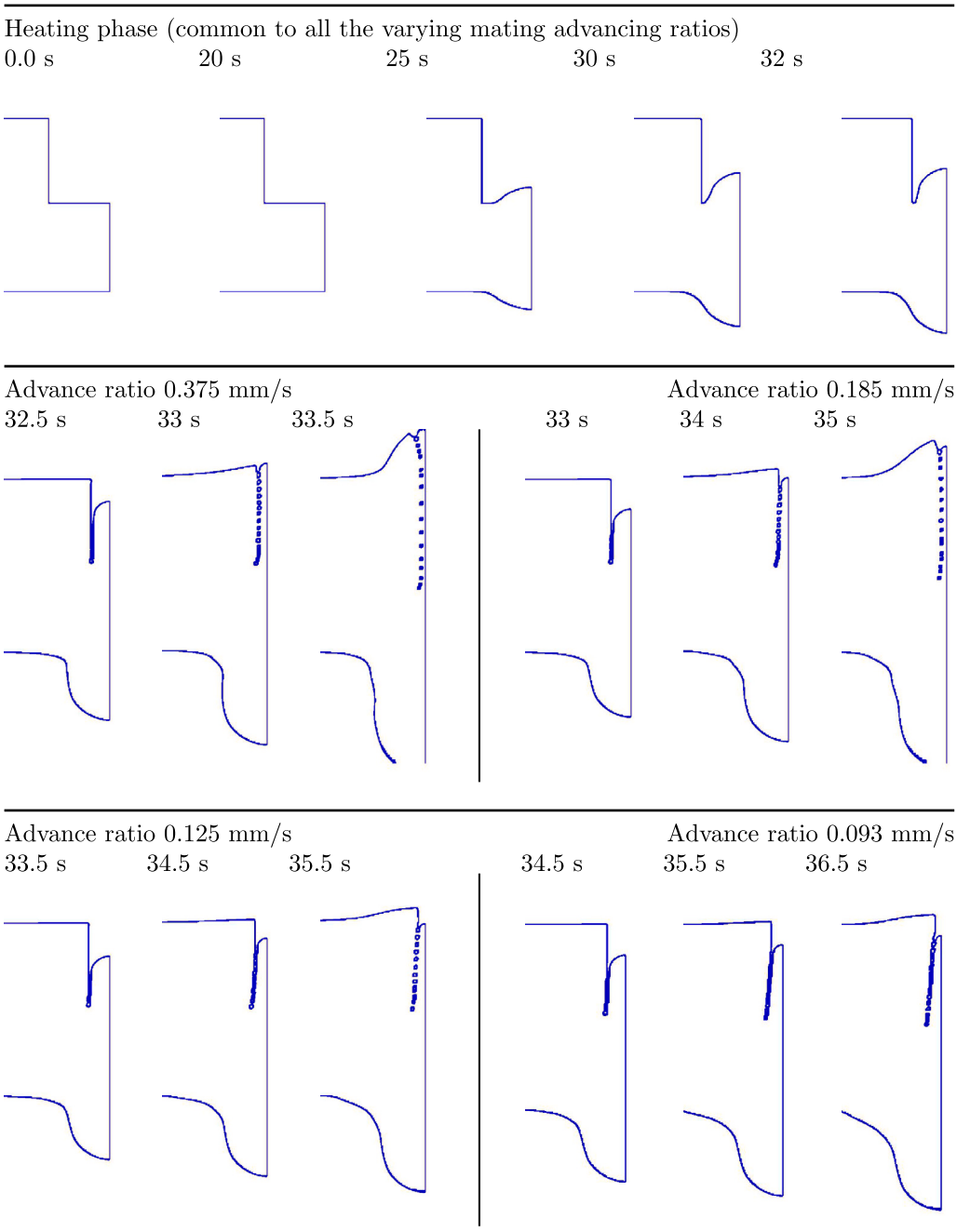

Fig. 8. Evolution of the free surface at selected times. Open condition.

Fig. 14 reports the comparison between the experimental and numerical cross-sections for the four wall positions. The comparison confirms the numerical model's ability to capture the complex interplay of material flow, temperature, and boundary constraints during the welding process. Overall, the validated numerical model demonstrates its reliability and predictive capability for analysing and optimising the butt-welding process in PVC profiles.

Conclusions

This study has provided a detailed exploration of the butt-joint welding process for PVC profiles, focusing on the complex interactions between heat transfer, viscoelastic deformation, and material flow. By developing and applying a multiphysics numerical model, we have gained valuable insights into the behaviour of PVC under welding conditions, as well as the factors influencing the quality of the final joint. It is important to remark that the quality of the welding is here intended from an aesthetic point of view. A "good weld" is one that keeps the molten PVC confined within the chamfered region, producing a clean joint that does not require post-weld trimming. This is the preferred outcome in industrial production because it provides a superior surface finish and avoids secondary operations. On the contrary a "bad weld" is one in which the molten PVC is not adequately confined during welding, producing an excessive external bead or protrusion to be removed by a dedicated trimming knife, inevitably leaving a visible mark on the frame surface.

One of the key findings is the critical role played by the thermal properties of PVC. Its low thermal conductivity results in steep temperature gradients during welding, making precise control of heating times and temperatures essential. Insufficient heating can leave the material too viscous to form an adequate weld, while excessive heating

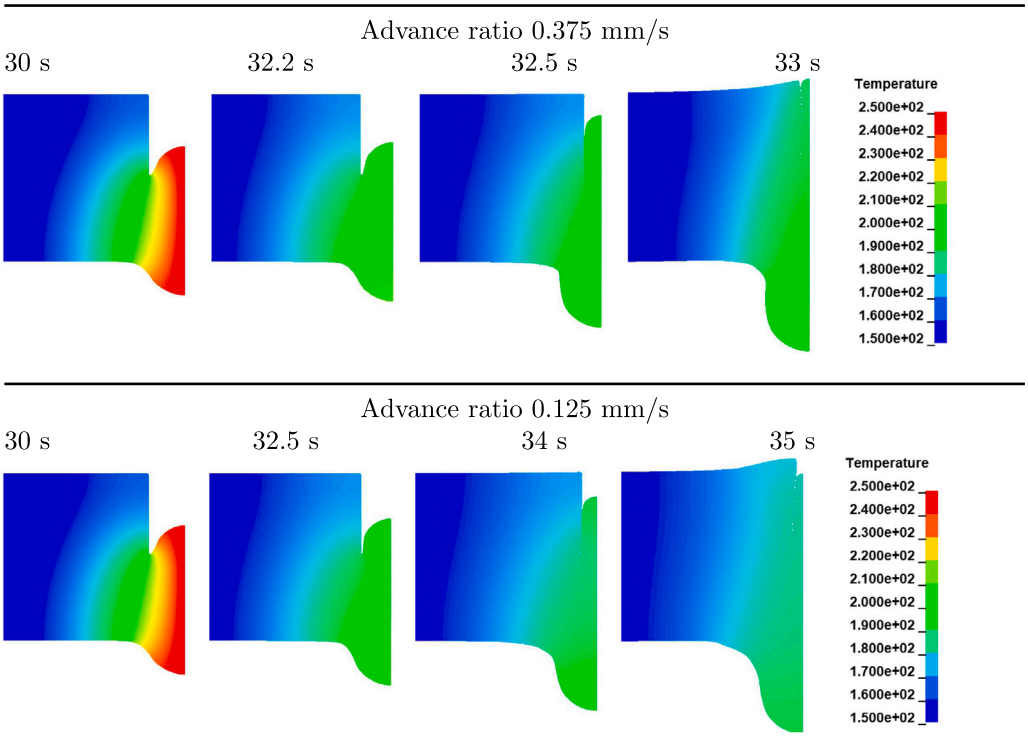

Fig. 9. Temperature distribution during the welding process for varying advancing ratios.

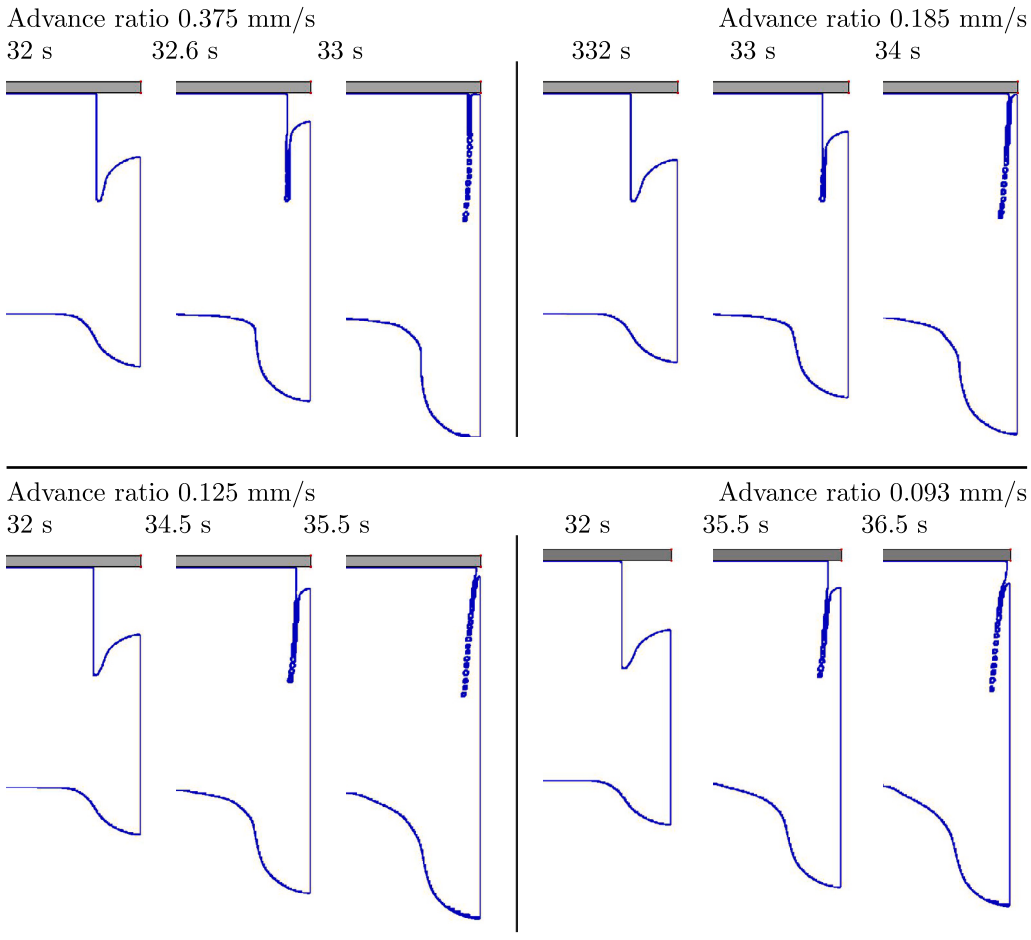

Fig. 10. Evolution of the free surface at selected times. Rigid wall condition.

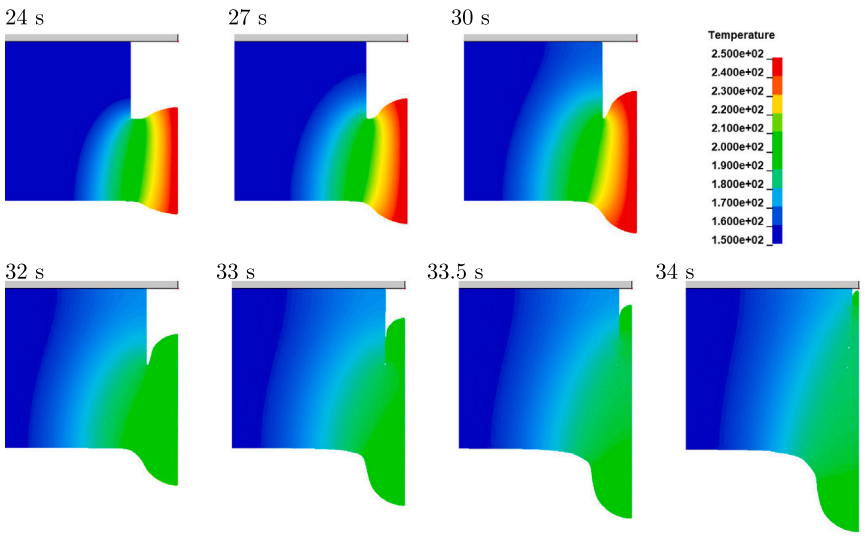

Fig. 11. Evolution of temperature during the welding process. Advancing ratio of 0.185 mm/s.

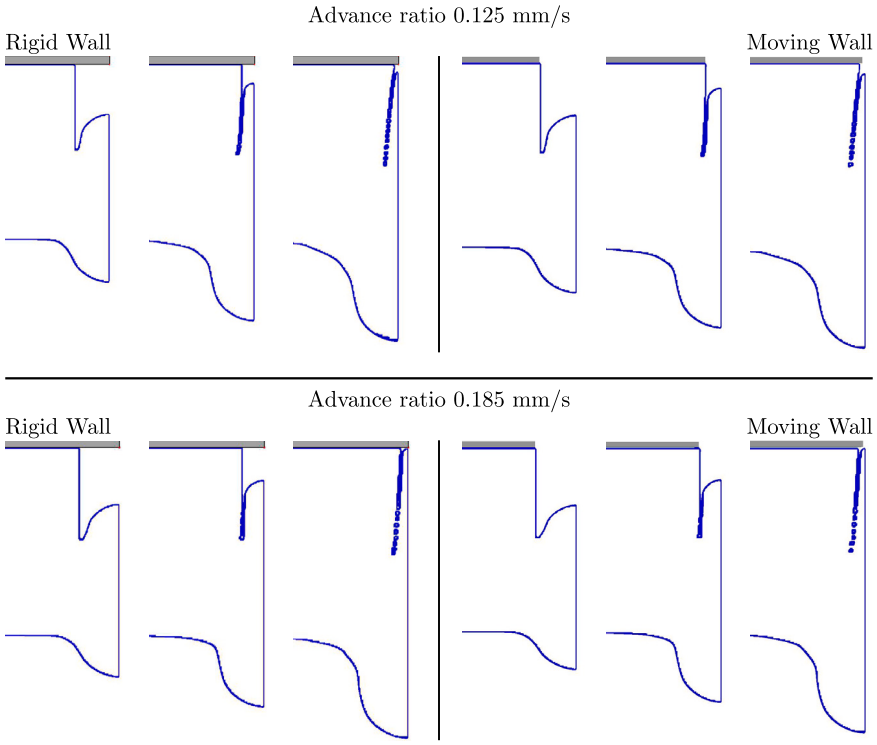

Fig. 12. Comparison of the evolution of the free surface at selected times for an advance ratio of 0.125 mm/s (top) and 0.185 mm/s (bottom) for the rigid wall (left) and moving wall (right) condition.

risks material degradation. The highly temperature-dependent viscosity of PVC further amplifies these challenges, as it dictates the material's ability to flow and fill the mating surface.

Mating velocity emerged as another significant factor influencing weld quality. Higher velocities promote better flow and fusion within the chamfer region, but they also increase the risk of material overflow, which can compromise the weld's appearance and require additional finishing. On the other hand, slower velocities allow the material to cool too much, leading to incomplete filling of the weld zone and potential functional weaknesses.

The geometry of the profiles and the presence of a rigid upper wall also play important roles. The rigid wall improves the weld's aesthetic quality by confining material flow and preventing excessive overflow. Functionally, however, the success of the weld remains dependent on maintaining the right balance of temperature and mating velocity, particularly in ensuring proper material flow within the chamfer region.

The numerical model was validated against experimental data obtained in collaboration with GRAF Synergy, whose support allowed modifications to industrial welding equipment for testing purposes. The agreement between the predicted and observed weld morphologies highlights the accuracy of the model. Nevertheless, it should be noted that some details of the welding process, such as exact mating velocities and heating times, remain proprietary, limiting the ability to share a complete dataset.

Overall, this study demonstrates the power of numerical simulations as a tool for understanding and optimising the welding process for

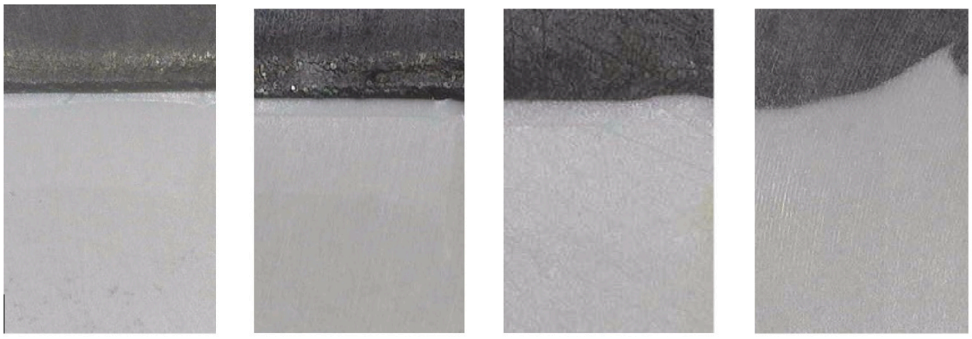

Fig. 13. Images of the experimental cross-sections of the welded profiles for varying moving blade distance from the chamfer edge: 0 mm, 0.3 mm, 0.5 mm, 2.5 mm, moving from the left image to the right.

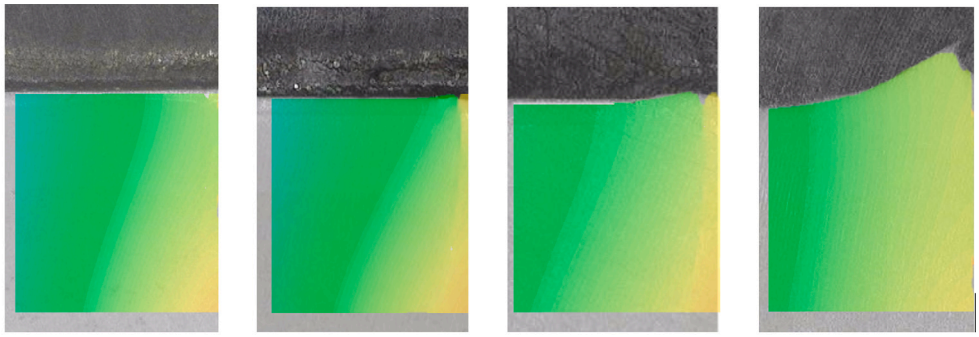

Fig. 14. Overlay of the numerical simulations on top of the experimental images.

thermoplastic materials. By capturing the intricate interplay of heat, material flow, and deformation, the model provides a reliable method for predicting the quality of welds and exploring the effects of different process parameters. The presented modelling approach helps to identify conditions under which bead formation can be controlled or suppressed, thus providing practical guidance for reducing secondary operations and improving weld aesthetics in industrial manufacturing. Eventually, the authors claim that the benefit of this numerical study is twofold:

(1) understanding and reproducing the physical behaviour of the butt-welding process by capturing the complex thermo-mechanical interactions occurring during PVC welding, including material flow, confinement, and bead formation;
(2) providing a tool for process optimisation: the model can be used to explore the influence of welding parameters (such as pressure, temperature, timing, chamfer geometry, and the position of the confining tool) on weld quality, offering a systematic and cost-effective way to identify process conditions under which the bead is minimised or suppressed.

Looking ahead, future work could expand on this foundation by incorporating additional complexities, such as multi-material interfaces or dynamic heating strategies. Extending the model to other thermoplastic materials and welding configurations could also enhance its industrial applicability, offering broader insights into the challenges and opportunities of thermoplastic welding.

CRediT authorship contribution statement

Riccardo Panciroli: Writing – review & editing, Writing – original draft, Methodology, Investigation, Conceptualization. **Daniele Chiappini:** Writing – review & editing, Visualization, Methodology, Conceptualization. **Roberto Palazzetti:** Writing – review & editing, Supervision, Investigation.

Declaration of competing interest

The authors declare that they have no known competing financial interests or personal relationships that could have appeared to influence the work reported in this paper.

Appendix A. Effect of advancing velocity during the heating phase

The mating velocity of the PVC profiles as they approach and contact the heating blade plays a critical role in shaping the morphology of the weld. Numerical simulations reveal that an increase in the mating velocity introduces a pronounced material whirl in the lower portion of the weld bead. This phenomenon arises due to the interaction between the advancing profiles and the viscous material near the melting temperature, combined with the geometric constraints of the chamfer and the heating blade.

As the mating velocity increases, the flowing material encounters greater resistance due to its inertia and the thermal gradients present within the molten zone. This resistance causes a portion of the molten material to form a circular flow pattern or "whirl" at the lower edge of the chamfer. The faster the profiles advance, the more pronounced and larger these whirls become. At very high velocities, the whirls exhibit increased size and rotational motion, effectively pushing molten material downward and away from the primary weld interface.

The lower portion of the weld, where these whirls occur, is hidden from view after the welding process is complete. Consequently, the aesthetic quality of the weld, often judged based on the visible upper surface, remains unaffected by this phenomenon. However, the whirls in the lower portion may influence the structural integrity of the weld. Excessive swirling can lead to material thinning in other regions of the weld bead or create small voids if the material flow is not uniform.

Fig. A.15 illustrates the development of material whirls at varying mating velocities. At lower velocities (left image), the molten material flows smoothly, forming a uniform bead without significant turbulence.

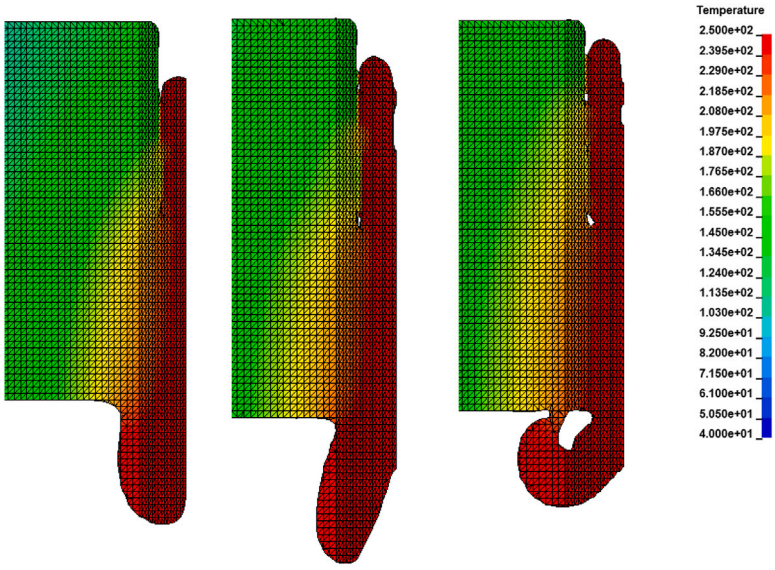

Fig. A.15. Visualisation of material flow patterns in the lower weld zone at varying mating velocities. At low mating velocities (left), the material flows smoothly without significant turbulence, resulting in a uniform weld bead. As the velocity increases (centre), pronounced whirls develop in the lower portion of the weld, characterised by circular flow patterns at the higher velocities (right).

In contrast, increasing the velocity (central and right images), the whirls become evident, characterised by circular flow patterns in the lower weld zone. These simulations underline the importance of carefully selecting the mating velocity to balance material flow uniformity with efficient process execution.

While the whirls in the lower weld zone are not directly visible, their presence highlights the importance of process optimisation. Operators must consider the trade-off between faster processing times and the potential for non-uniform material distribution in the weld bead. For applications where the weld's structural integrity is critical, slower mating velocities may be preferred to minimise the formation of whirls and ensure consistent bonding across the entire weld.

This observation further underscores the utility of the numerical model in providing detailed insights into the hidden aspects of the welding process, enabling informed decisions to enhance both the functional and aesthetic outcomes of the weld.

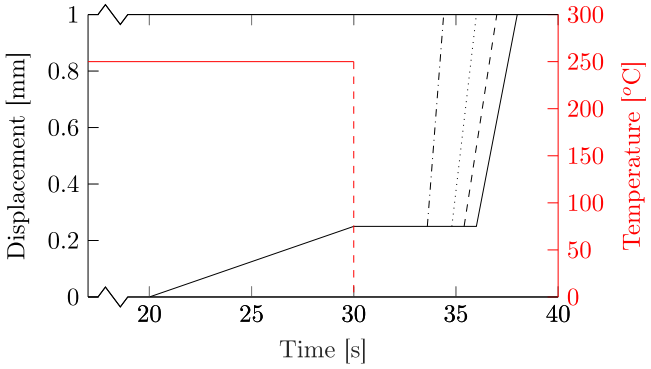

Fig. B.16. Optimal combination of prescribed mating velocity and dwell time. Solid, dashed, dotted, and dashdotted lines correspond to a final advancing ratios of 0.375, 0.465, 0.625, and 0.950 mm/s, respectively.

Appendix B. Optimal combination of dwell time and mating velocity

In this section, we focus on the configuration illustrated in Fig. 7, which includes the presence of a moving containment blade (considered as a moving rigid wall). In addition to the results presented in the main body of the paper, a further parametric investigation was conducted to evaluate the combined effect of dwell time—the pause between the removal of the heating blade and the initiation of the mating motion—and mating velocity on the final quality of the weld. This appendix summarises the outcome of that extended analysis, with a focus on identifying the optimal combination of parameters for producing a structurally sound and visually acceptable weld.

The study involved a matrix of simulations, varying the mating velocity across a broad range and coupling it with different dwell durations. While numerous cases were examined, only the most successful combination is reported here for brevity and clarity. The criterion for selecting the optimal case was based on two main quality indicators of the final welding cross-section: absence of polymer overflow on the top surface, thus eliminating the need for secondary machining, and lack of cold-welding regions, i.e., zones where the temperature during mating dropped below the critical threshold for adequate material fusion.

An interesting and practically significant outcome of this parametric analysis is the identification of a clear inverse relationship between mating velocity and optimal dwell time. Specifically, the faster the mating velocity, the shorter the dwell time should be in order to achieve an optimal weld. This trend is governed by two concurrent physical effects: higher mating velocities induce greater shear rates, which enhance the flow of the molten polymer and improve fusion quality; at the same time, shorter dwell times minimise thermal losses after blade removal, preserving a higher temperature and thus lower viscosity in the mating region.

This insight emerged from a systematic optimisation study involving four different mating velocities: 0.950 mm/s, 0.625 mm/s, 0.465 mm/s, and 0.375 mm/s. For each case, the dwell time was adjusted to identify the combination that resulted in the best welding outcome, defined as a weld free of top surface overflow and devoid of cold-welded regions—i.e., areas where the temperature had dropped below the threshold required for effective polymer bonding. The optimal parameters are summarised in the load histories schematically presented in Fig. A.15.

Of particular interest is the result for the 0.375 mm/s velocity, which was also analysed in the main body of the manuscript. In that initial analysis, the weld quality at this velocity was found to be unsatisfactory due to excessive flow in the upper region of the joint. However, the extended parametric study now reveals that this deficiency was

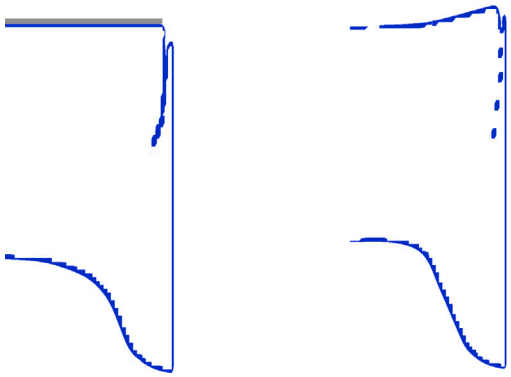

Fig. B.17. Evolution of the free surface in the last portion of the welding process. Moving boundary (left) vs Open condition (right).

not inherently due to the velocity itself, but rather to an insufficient dwell time prior to mating. When paired with an appropriately longer dwell time, the 0.375 mm/s case produces a weld with excellent surface morphology and internal cohesion, thereby validating the importance of synchronising thermal and kinematic parameters.

It is worth noting that, regardless of the specific mating velocity studied in this work, the fundamental physics governing weld quality remain unchanged. In all cases, the confinement of the molten PVC during the mating phase is primarily dictated by the presence of the backward-facing surface of the opposing profile. This surface consistently acts as a physical barrier, effectively containing the flow of the low-viscosity material and guiding it into the chamfer region. As such, it plays a critical role in shaping the final morphology of the weld, ensuring material redistribution occurs within the joining interface rather than escaping undesirably from the weld zone. Fig. B.17 provides a representative example of the material behaviour during the final stage of the welding process, highlighting the role of the backward-facing vertical surface in confining the molten polymer. This confinement effect is clearly observed when a moving barrier is employed, as the surface effectively redirects the material into the chamfer region. Conversely, in the absence of any confinement system, this guiding mechanism does not manifest, leading to unregulated material flow through the upper surface.

Overall, these findings underscore the capability of the numerical model not only to replicate complex physical behaviours but also to serve as a powerful optimisation tool for process design. By varying and analysing combinations of key parameters, the model provides guidance for achieving high-quality welds under a range of practical conditions.

To further assess the effectiveness of boundary constraints, the simulations were also repeated without any containment features such as the rigid stationary or moving wall. These cases allowed for a direct comparison, isolating the contribution of the mechanical confinement to the quality of the final weld. This complementary study underscores the importance of precise synchronisation between thermal and mechanical parameters and confirms the utility of dynamic confinement strategies in advanced welding processes.

Data availability

Data will be made available on request.

References

Alexandrou, A.N., McGilvreay, T.M., Burgos, G., 2001. Steady Herschel–Bulkley fluid flow in three-dimensional expansions. J. Non-Newton. Fluid Mech. 100 (1–3), 77–96.

Altinkaynak, A., Gupta, M., Spalding, M., Crabtree, S., 2011. Melting in a single screw extruder: Experiments and 3D finite element simulations. Int. Polym. Process. http://dx.doi.org/10.3139/217.2419.

Bhudolia, S., Gohel, G., Leong, K., 2020. Advances in ultrasonic welding of thermoplastic composites : A review. Materials 13, 1284–1310.

Bovo, E., Pieressa, A., Sorgato, M., Lucchetta, G., 2024. The influence of material properties and process parameters on energy consumption during extrusion of flexible PVC. Sustain. Mater. Technol. 39, http://dx.doi.org/10.1016/j.susmat.2023.e00782.

Braess, H., Wriggers, P., 2000. Arbitrary Lagrangian Eulerian finite element analysis of free surface flow. Comput. Methods Appl. Mech. Engrg. 190 (1–2), 95–109. http://dx.doi.org/10.1016/S0045-7825(99)00416-8.

Cao, W., Shen, Y., Wang, P., Yang, H., Zhao, S., Shen, C., 2019. Viscoelastic modeling and simulation for polymer melt flow in injection/compression molding. J. Non-Newton. Fluid Mech. 274 (September), 104186. http://dx.doi.org/10.1016/j.jnnfm.2019.104186.

Chiang, H., Hieber, C., Wnag, K., 1991. A unified simulation of the filling and postfilling stages in injection molding. Part I: Formulation. Polym. Eng. Sci. 31 (2).

Iftikhar, S., Mourad, A., Guessoum, M., 2022. Numerical modeling of friction stir welding of thermoplastic materials - An overview. In: 2022 Advances in Science and Engineering Technology International Conferences, ASET 2022. IEEE, http://dx.doi.org/10.1109/ASET53988.2022.9735017.

Jin, X., Heepe, L., Strueben, J., Adelung, R., Gorb, S., Staubitz, A., 2014. Challenges and solutions for joining polymer materials. Macromol. Rapid Commun. 35 (18), 1551–1570. http://dx.doi.org/10.1002/marc.201400200.

Kök, M., Demirelli, K., Aydogdu, Y., Kok, M., Demrelli, K., 2008. Thermophysical Properties Of Blend Of Poly (Vinyl Chloride) With Poly (Isobornyl Acrylate) Comparison of the transformation temperature, microstructure and magnetic properties of Co-Ni-Al and Co-Ni-Al-Cr shape memory alloys View project Shape Memory A. Technical Report.

Moreno, E., Larese, A., Cervera, M., 2016. Modelling of Bingham and Herschel-Bulkley flows with mixed P1/P1 finite elements stabilized with orthogonal subgrid scale. J. Non-Newton. Fluid Mech. 228, 1–16. http://dx.doi.org/10.1016/j.jnnfm.2015.12.005.

Münstedt, H., 1977. Relationship between rheological properties and structure of poly (vinyl chloride). J. Macromol. Sci. Part B 14 (2), 195–212. http://dx.doi.org/10.1080/00222347708220364.

Münstedt, H., 2021. Rheological measurements and structural analysis of polymeric materials. Polymers 13 (7), http://dx.doi.org/10.3390/polym13071123.

Nakayama, Y., 2018. Chapter 2 - characteristics of a fluid. In: Nakayama, Y. (Ed.), Introduction To Fluid Mechanics, second ed. Butterworth-Heinemann, pp. 9–24. http://dx.doi.org/10.1016/B978-0-08-102437-9.00002-4.

Nisar, J., Khan, M.S., Iqbal, M., Shah, A., Ali, G., Sayed, M., Khan, R.A., Shah, F., Mahmood, T., 2018. Thermal decomposition study of polyvinyl chloride in the presence of commercially available oxides catalysts. Adv. Polym. Technol. 37 (6), 2336–2343. http://dx.doi.org/10.1002/adv.21909.

Silva, L.R., Marques, E.A., da Silva, L.F., 2021. Polymer joining techniques state of the art review. Weld. the World 65 (10), 2023–2045. http://dx.doi.org/10.1007/s40194-021-01143-x.

Snoeijer, J.H., Pandey, A., Herrada, M.A., Eggers, J., 2020. The relationship between viscoelasticity and elasticity: Viscoelasticity and elasticity. Proc. R. Soc. A: Math. Phys. Eng. Sci. 476 (2243), http://dx.doi.org/10.1098/rspa.2020.0419.

Tomaszewska, J., Sterzyński, T., Woźniak-Braszak, A., Banaszak, M., 2021. Review of recent developments of glass transition in pvc nanocomposites. Polymers 13 (24), http://dx.doi.org/10.3390/polym13244336.

Tutunjian, S., Eroglu, O., Dannemann, M., Modler, N., Fischer, F., 2020. A numerical analysis of an energy directing method through friction heating during the ultrasonic welding of thermoplastic composites. J. Thermoplast. Compos. Mater. 33 (11), 1569–1587. http://dx.doi.org/10.1177/0892705719833108.

Van De Ven, J.D., Erdman, A.G., 2007a. Bridging gaps in laser transmission welding of thermoplastics. J. Manuf. Sci. Eng. 129 (6), 1011–1018. http://dx.doi.org/10.1115/1.2769731.

Van De Ven, J., Erdman, A., 2007b. Hot pin welding of thin poly(vinyl chloride) sheet. J. Vinyl Addit. Technol. 13 (2), 110–115. http://dx.doi.org/10.1002/vnl.20111.

Van De Ven, J., Erdman, A., 2007c. Laser transmission welding of thermoplastics - Part I: Temperature and pressure modeling. J. Manuf. Sci. Eng. 129 (5), 849–858. http://dx.doi.org/10.1115/1.2752527.

Van De Ven, J.D., Erdman, A.G., 2007d. Laser transmission welding of thermoplastics - Part II: Experimental model validation. J. Manuf. Sci. Eng. 129 (5), 859–867. http://dx.doi.org/10.1115/1.2752832.

Vendan, S.A., Natesh, M., Garg, A., Gao, L., 2019. Polymer welding techniques and its evolution. In: Confluence of Multidisciplinary Sciences for Polymer Joining. Springer Singapore, pp. 11–71. http://dx.doi.org/10.1007/978-981-13-0626-6{_}2.

Zhang, Z., Wang, X., Luo, Y., Zhang, Z., Wang, L., 2010. Study on heating process of ultrasonic welding for thermoplastics. J. Thermoplast. Compos. Mater. 23 (5), 647–664. http://dx.doi.org/10.1177/0892705709356493.